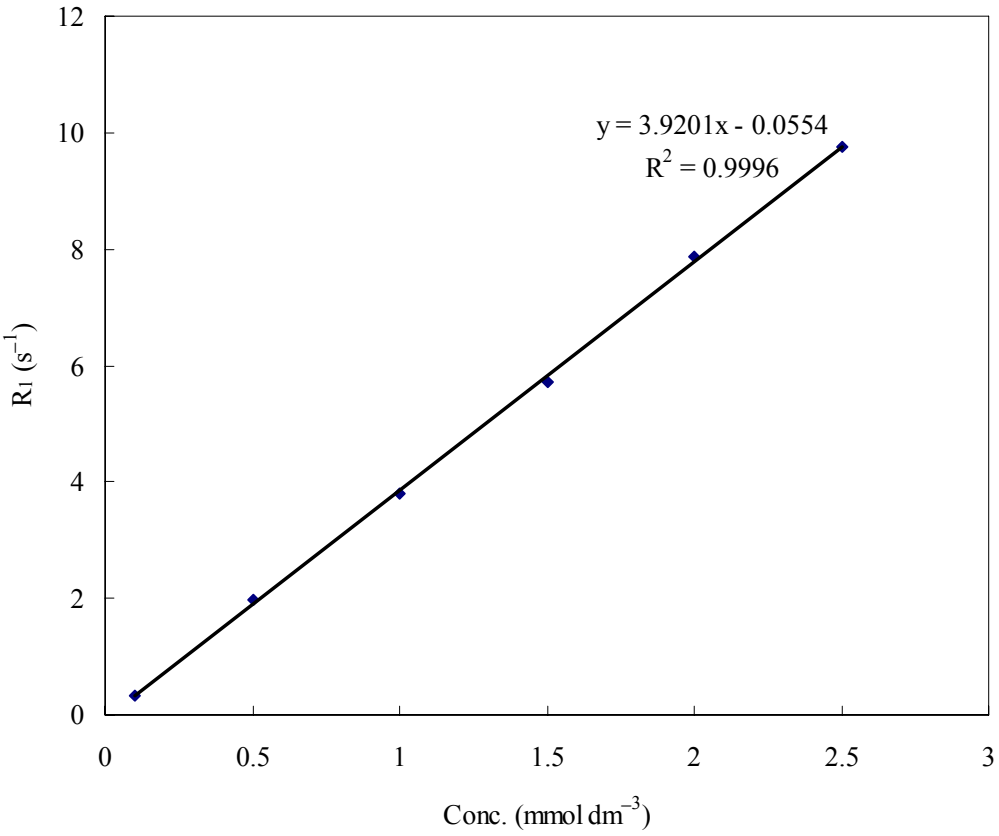

Figure 1S The plot of the relaxation rate *vs.* concentration of [Gd(TTDA-BMA)(H_2O)].

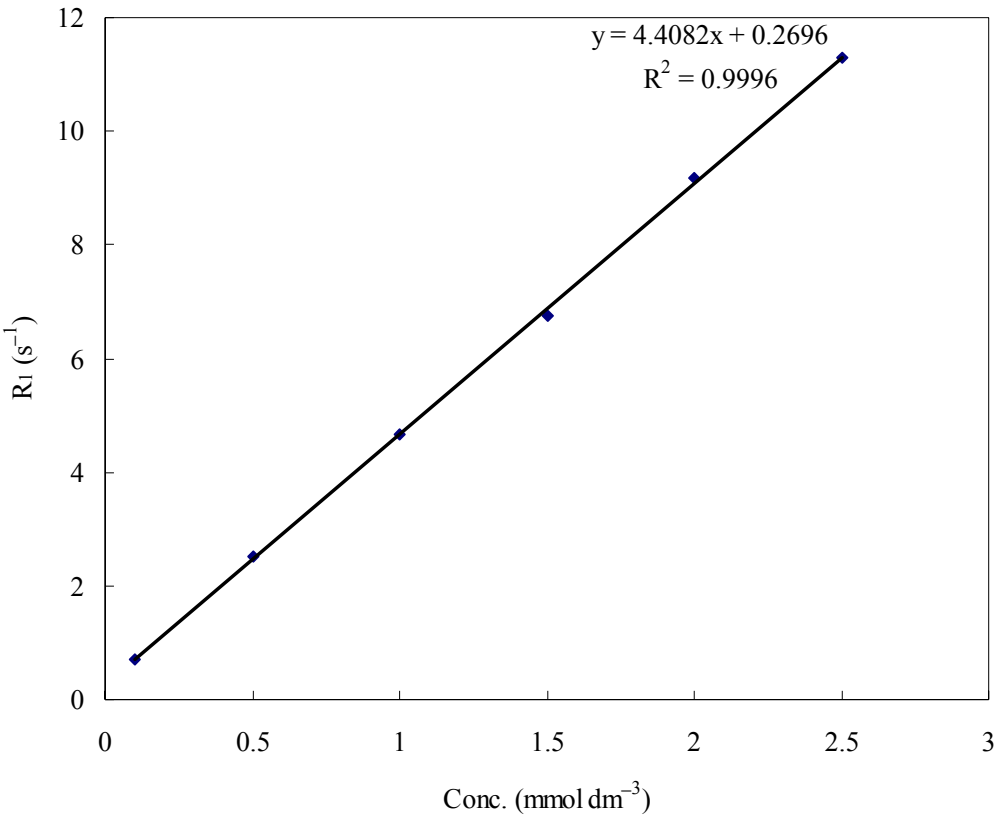

Figure 2S The plot of the relaxation rate *vs.* concentration of [Gd(TTDA-BBA)(H_2O)].

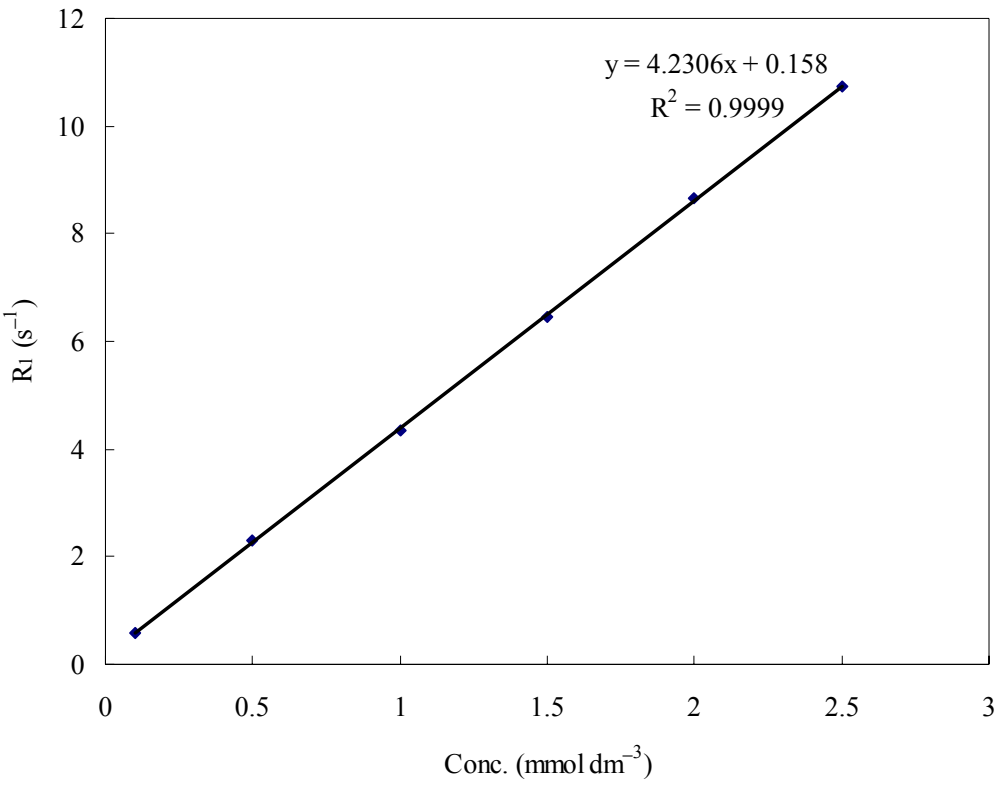

Figure 3S The plot of the relaxation rate *vs.* concentration of $[Gd(TTDA\text{-}N\text{-}MOBA)(H_2O)]^-$.

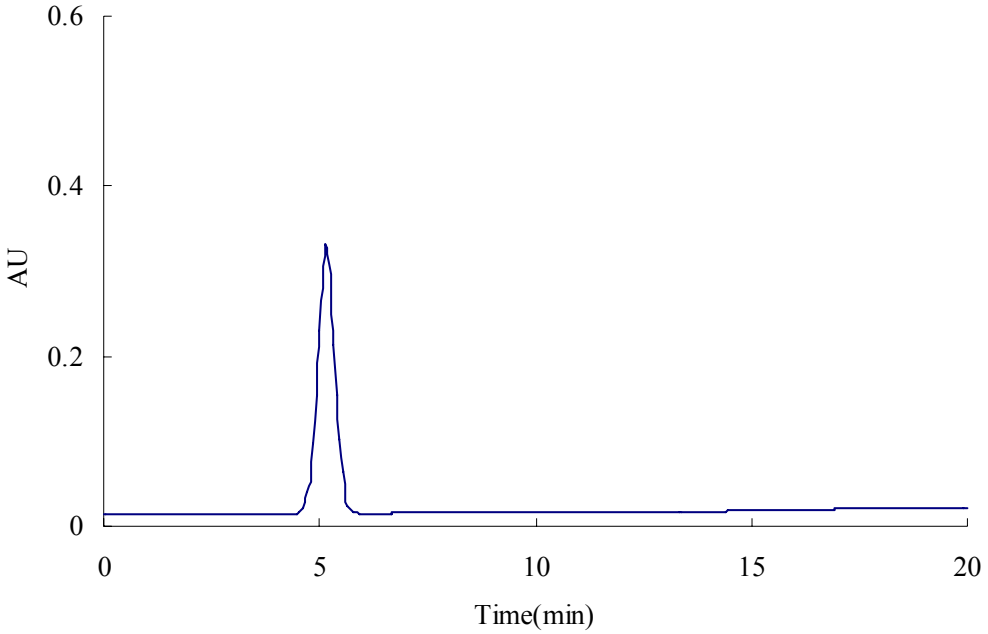

Figure 4S HPLC analysis of TTDA-BMA (reverse-phase C18 column); HPLC conditions: gradient of 0 to 100 % MeOH using 0.1 % TFA in water as aqueous phase; flow rate: 0.5 mL/min; the wavelength set at 280 nm.

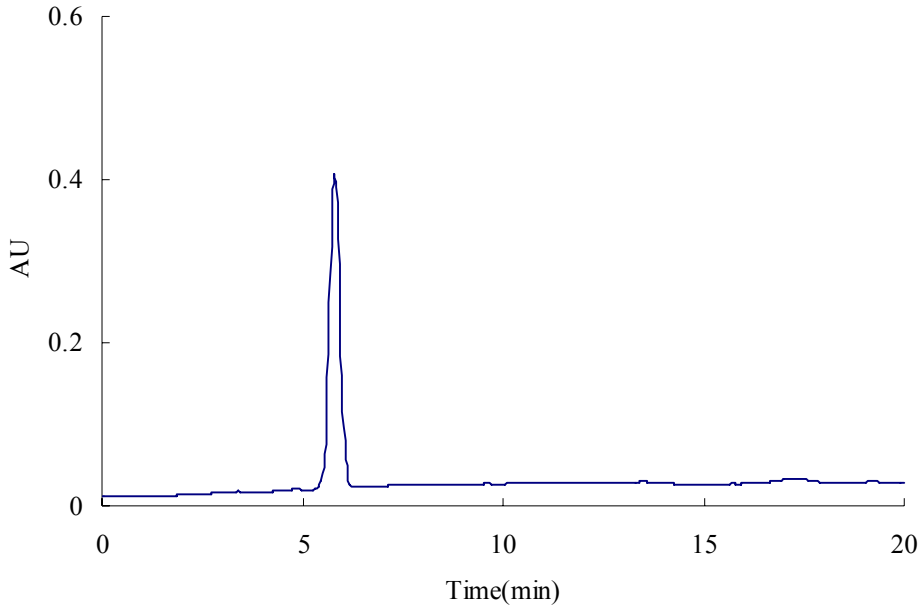

Figure 5S HPLC analysis of TTDA-BBA (reverse-phase C18 column); HPLC conditions: gradient of 0 to 100 % MeOH using 0.1 % TFA in water as aqueous phase; flow rate: 0.5 mL/min; the wavelength set at 280 nm.

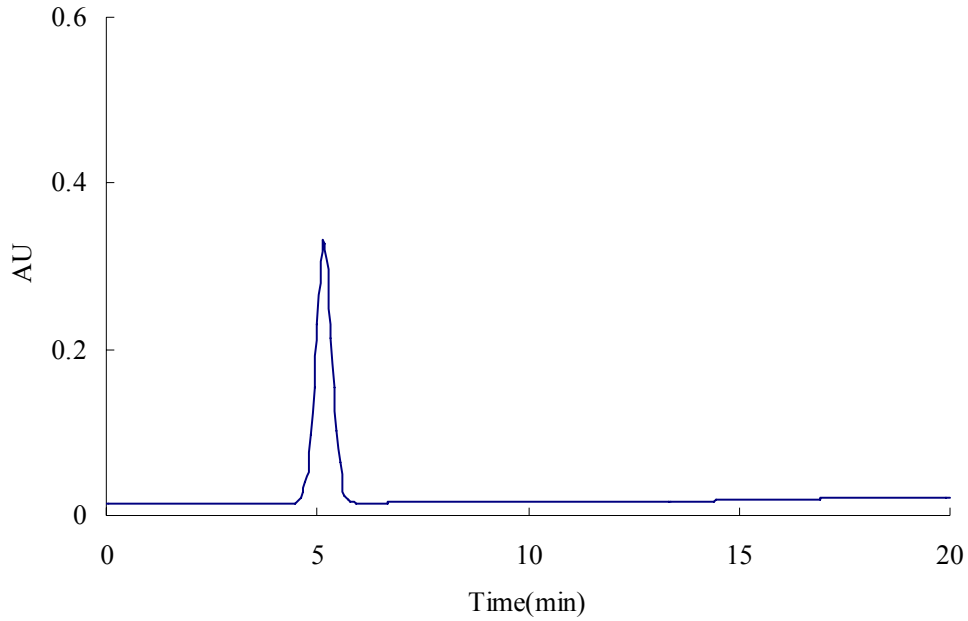

Figure 6S HPLC analysis of TTDA-*N*-MOBA (reverse-phase C18 column); HPLC conditions: gradient of 0 to 100 % MeOH using 0.1 % TFA in water as aqueous phase; flow rate: 0.5 mL/min; the wavelength set at 280 nm.

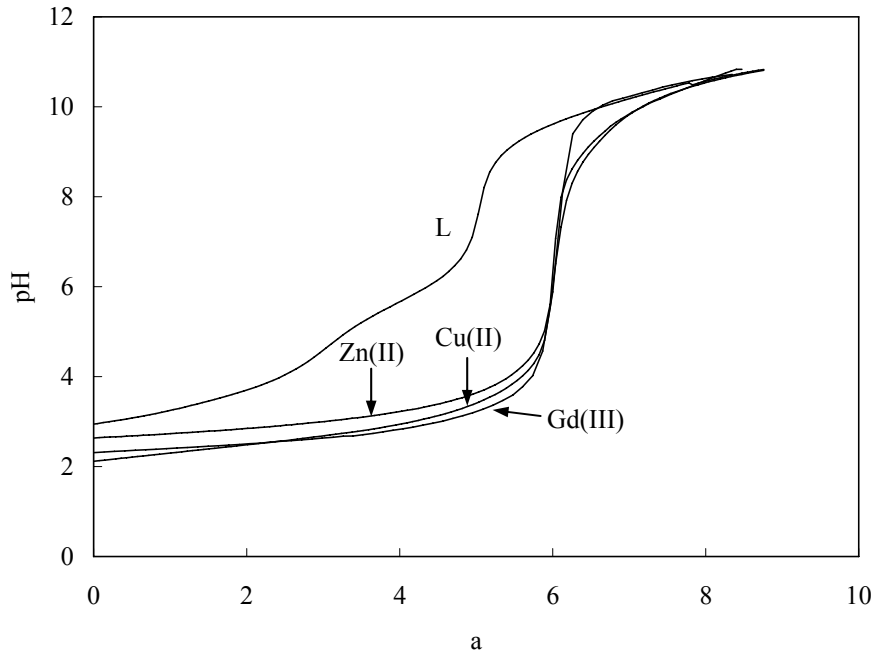

Figure 7S Titration curves for 1:1 ratios of metal ion to TTDA-BMA, I = 0.1 mol dm^{-3} Me_4NCl; T = 25.0 ± 0.1 °C; concentrations of ligand and metal ions = 1.0×10^{-3} mol dm^{-3}.

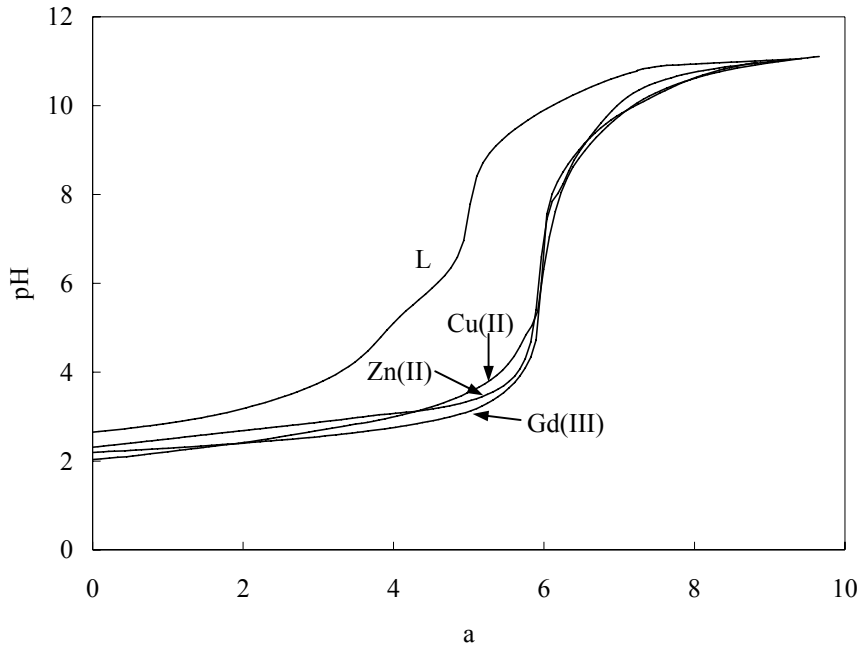

Figure 8S Titration curves for 1:1 ratios of metal ion to TTDA-BBA, I = 0.1 mol dm^{-3} Me_4NCl; T = 25.0 ± 0.1 °C; concentrations of ligand and metal ions = 1.0×10^{-3} mol dm^{-3}.

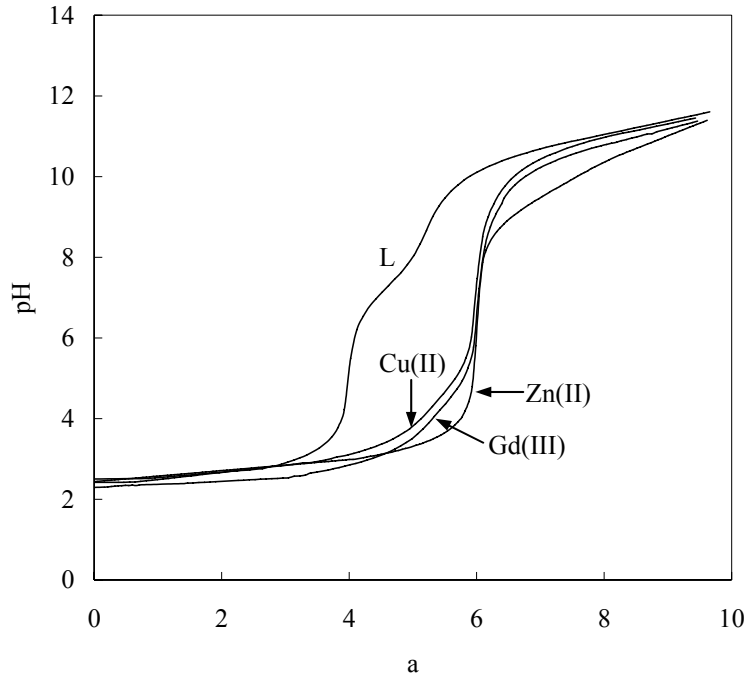

Figure 9S Titration curves for 1:1 ratios of metal ion to TTDA-*N*-MOBA, I = 0.1 mol dm^{-3} Me_4NCl; T = 25.0 ± 0.1 °C; concentrations of ligand and metal ions = 1.0×10^{-3} mol dm^{-3}.

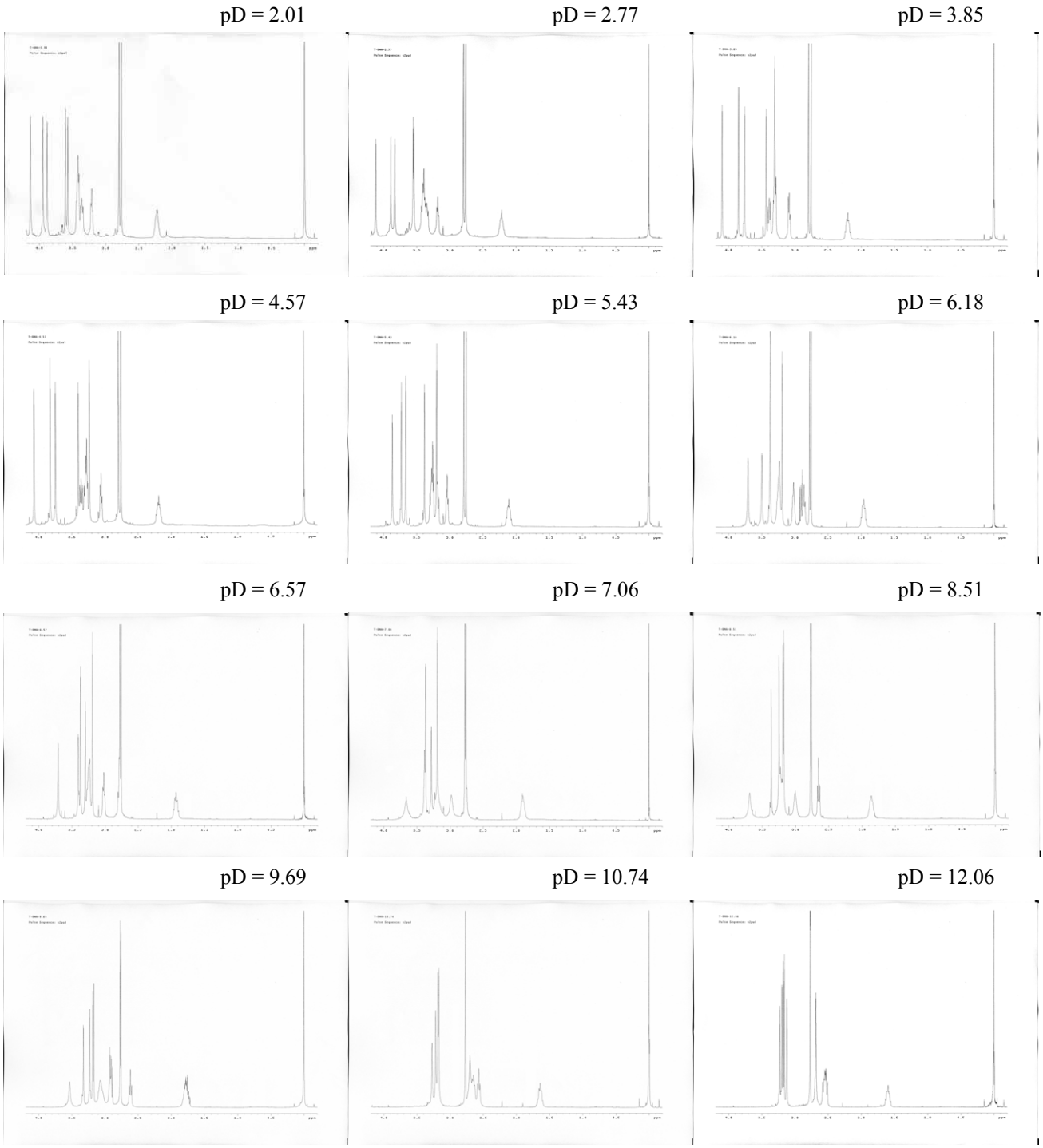

Figure 10S ^{1}H-NMR spectra of TTDA-BMA as a function of pD.

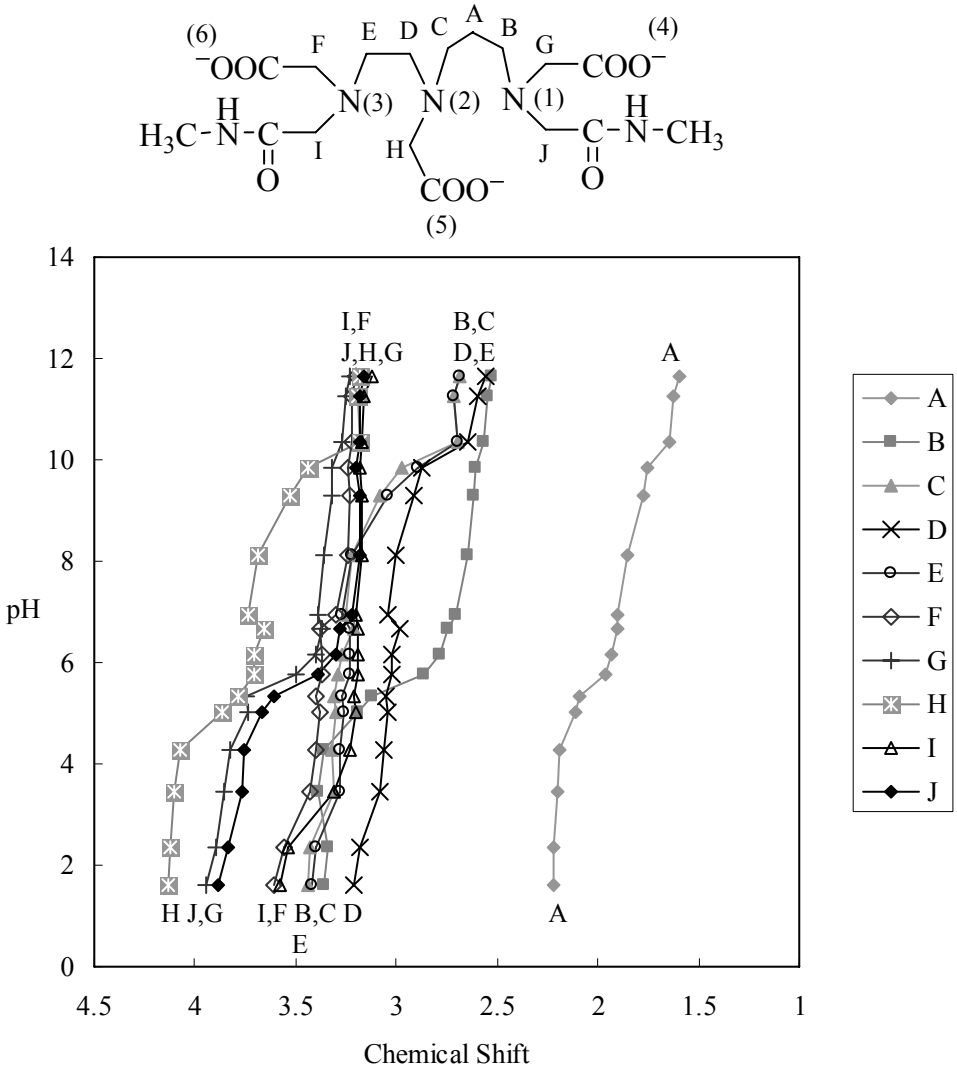

Figure 11S Proton NMR titration curves for TTDA-BMA.

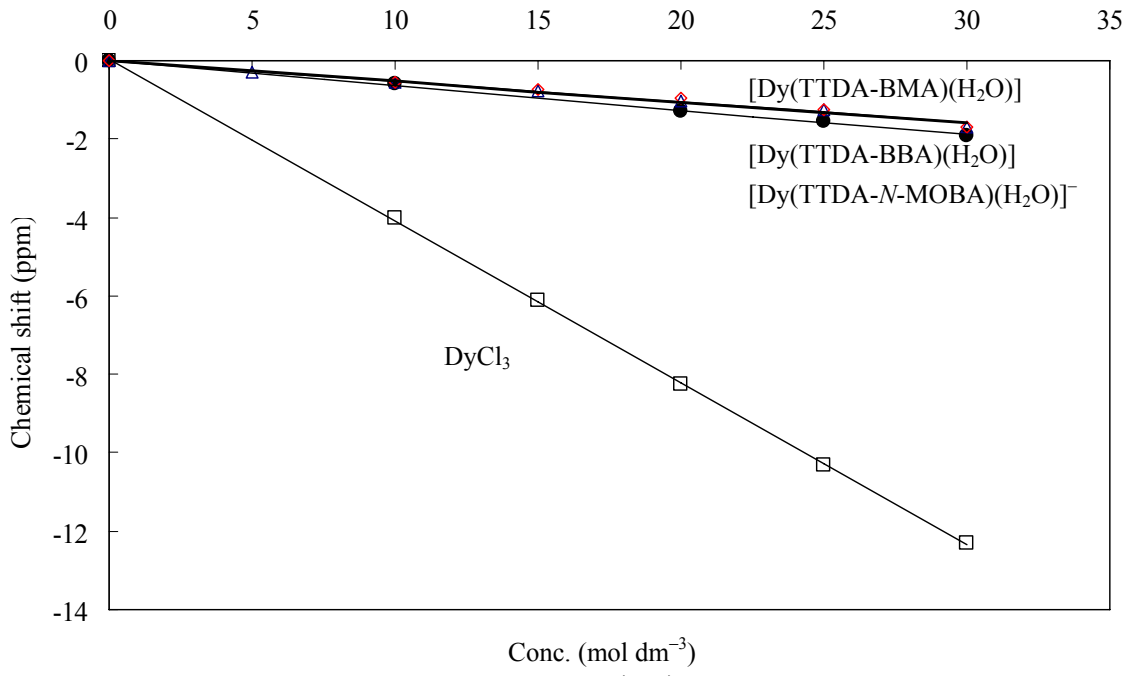

Figure 12S The Dy(III)-induced water ^{17}O-NMR shift versus Dy(III) chelate concentration for solution of $DyCl_3$ (□), [Dy(TTDA-BMA)(H_2O)] (Δ), [Dy(TTDA-BBA)(H_2O)] (◊) and [Dy(TTDA-*N*-MOBA)(H_2O)]$^-$ (•) in D_2O at 25.0 ± 0.1 °C.

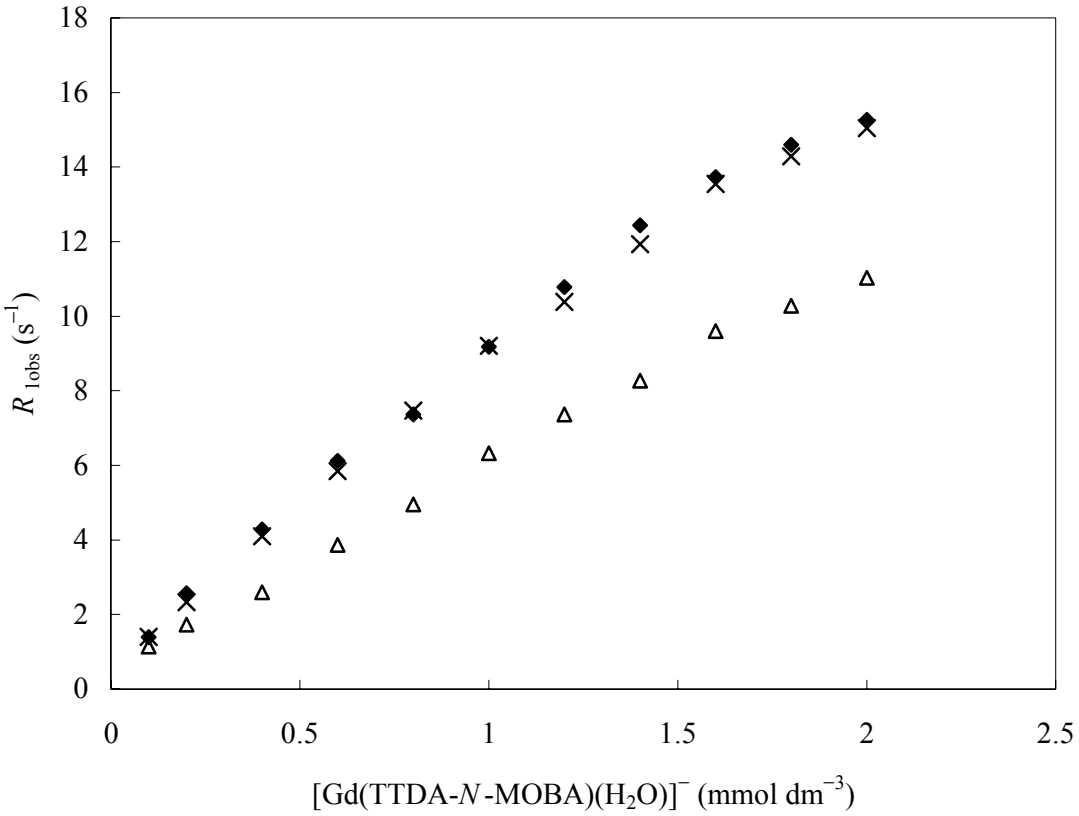

Figure 13S Water proton relaxation rates of aqueous solutions for the binding to 0.6 mmol dm^{-3} HSA of [Gd(TTDA-*N*-MOBA)(H_2O)]$^-$ alone (♦) or in combination with displacer drugs [ibuprofen 0.6 mmol dm^{-3} (×); warfarin 0.6 mmol dm^{-3} (Δ)] measured at 20 MHz, 25.0 ± 0.1 °C, 50 mmol dm^{-3} phosphate buffer at pH 7.4.

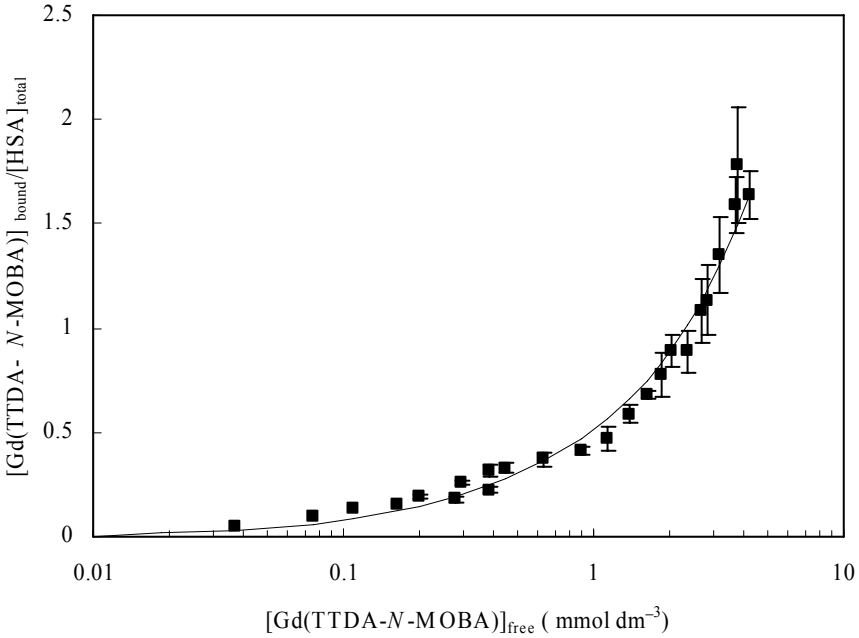

Figure 14S Binding isotherm for [Gd(TTDA-*N*-MOBA)(H_2O)] (37.0 ± 0.1 °C, phosphate buffer, pH 7.4) to 4.5% (w/v) HSA.

Table 1S Percent protonation fractions of the different basic sites of TTDA-BMA, DTPA-BMA, DTPA and TTDA for different values of *n*

Ligand	f_1	f_2	f_3	f_4	f_5	f_6
TTDA-BMA						
$n = 1$	13.1	69.1	17.7	0	0	0
$n = 2$	71.7	74.3	21.8	0	32.1	0
$n = 3$	92.1	86.4	47.4	0	74.2	0
DTPA-BMA [a]						
$n = 1$	11	78	11	0	0	-
$n = 2$	61	58	61	0	20	-
DTPA [b]						
$n = 1$	26	41	26	0	0	-
$n = 2$	87	16	87	5	0	-
$n = 3$	80	64	80	0	76	-
TTDA [c]						
$n = 1$	27.4	50.9	19.2	0	0	-
$n = 2$	89.9	41.0	69.0	0	0	-
$n = 3$	99.5	93.1	95.1	–3.3	25.0	-

[a] Reference 1. [b] Reference 2. [c] Reference 3.

Table 2S Lifetimes of the Eu(III) excited levels (τ, ms) and number of coordinated water molecules (q) obtained in 1×10^{-3} mol dm^{-3} H_2O and D_2O solutions of [Eu(TTDA-BMA)(H_2O)], [Eu(TTDA-BBA)(H_2O)] and [Eu(TTDA-*N*-MOBA)(H_2O)]$^-$.

	[Eu(TTDA-BMA)(H_2O)]	[Eu(TTDA-BBA)(H_2O)]	[Eu(TTDA-*N*-MOBA)(H_2O)]$^-$
τ_{H_2O}	0.60	0.47	0.61
τ_{D_2O}	1.74	1.11	1.87
q^a	1.14	1.27	1.17
q^b	1.01	1.15	1.04

[a]The q value was determined by equation (1S). [b]By equation (2S).

Table 3S Temperature dependence of reduced transverse and longitudinal ^{17}O relaxation rates and reduced angular frequencies of solutions containing [Gd(TTDA-BMA)(H_2O)] at 9.4 T. (c = 0.054 mol kg^{-1}, pH = 5.6)

1000K/T	$\ln(1/T_{2r})$	$\ln(1/T_{1r})$	$\Delta\omega_r/10^6$ rad s^{-1}
3.595	14.166	11.071	-0.384
3.531	14.171	10.814	-0.476
3.411	14.022	10.371	-0.676
3.224	13.600	9.722	-0.861
3.047	13.078	9.305	-0.784
2.957	12.716	9.047	-0.738
2.872	12.250	8.823	-0.722

Table 4S Temperature dependence of reduced transverse and longitudinal ^{17}O relaxation rates and reduced angular frequencies of solutions containing [Gd(TTDA-BBA)(H_2O)] at 9.4 T. (c = 0.053 mol kg^{-1}, pH = 5.2)

1000K/T	$\ln(1/T_{2r})$	$\ln(1/T_{1r})$	$\Delta\omega_r/10^6$ rad s^{-1}
3.595	14.143	11.152	-0.461
3.531	13.998	10.959	-0.553
3.411	13.909	10.591	-0.604
3.224	13.491	9.870	-0.720
3.047	12.969	9.319	-0.709
2.957	12.649	9.121	-0.697
2.872	12.345	8.806	-0.669

Table 5S Temperature dependence of reduced transverse and longitudinal ^{17}O relaxation rates and reduced angular frequencies of solutions containing $[Gd(TTDA\text{-}N\text{-}MOBA)(H_2O)]^-$ at 9.4 T. (c = 0.048 mol kg^{-1}, pH = 5.5)

1000K/T	$\ln(1/T_{2r})$	$\ln(1/T_{1r})$	$\Delta\omega_r/10^6$ rad s^{-1}
3.595	13.620	10.802	-0.769
3.531	13.608	10.672	-0.845
3.411	13.517	10.428	-0.922
3.224	13.100	10.026	-0.809
3.047	12.531	9.245	-0.692
2.957	12.193	8.942	-0.672
2.872	11.724	8.818	-0.634

S1 ^{1}H NMR titrations. The observed deshielding of the methylene protons of the ligand is correlated with the percentages of protonation of the amino or carboxylate groups.[1, 2] The protonation fractions of TTDA-BMA (%) are compared with other ligands (Table 1S). The f_j values for the nitrogen atoms (f_1, f_2 and f_3) and carboxylate groups (f_4, f_5 and f_6) labelled in Figure 8S were calculated for integer values of n (1–3, number of moles of acid added per mole of polyaminopolycarboxylate). When 1 equivalent of acid is added to the fully unprotonated form of the ligand, the f_j values for TTDA-BMA (n = 1, f_1 = 13.1, f_2 = 69.1, f_3 = 17.7) are similar to that of DTPA-BMA (n = 1, f_1 = 11, f_2 = 78, f_3 = 11). For the TTDA and DTPA-bis(amide) derivatives, the preference of the first protonation (n = 1) for the central nitrogen is higher than that of the terminal nitrogen. These results indicate that the central nitrogen is more strongly basic than those of terminal nitrogen atoms. For n > 1 the protonation fraction values obtained for TTDA-BMA are as follows: at n = 2 (f_1 = 71.7, f_2 = 74.3, f_3 = 21.8, f_5 = 32.1) and at n = 3 (f_1 = 92.1, f_2 = 86.4, f_3 = 47.4, f_5 = 74.2). There is a preference for the terminal propylene and central nitrogens (site 1 and 2) relative to the ethylene nitrogen for n = 2. At n = 3, the protons migrate to amine nitrogens and to one of the carboxylate oxygens. Moreover, the percent protonation fraction of TTDA-BMA is similar to that of DTPA when n = 3. Calculated values of f_1, f_2, f_3 and f_5 in Table 1S indicate that the terminal propylene and central nitrogen atoms and the middle carboxylate group (site 5) undergo the greatest increases in protonation during this step.

S2 Conditional stability constant and pM values. The conditional stability constant of a metal chelate ($K_{ML(cond)}$) under physiological condition (pH 7.4) is more important than the thermodynamic stability constant for biological studies. The former literature shows the extent of metal chelation at pH 7.4 and can be expressed by eq 3 [4]

$$K_{ML(cond)} = K_{ML(therm)}(1 + K_1[H^+] + K_1K_2[H^+]^2 + ...)^{-1} \qquad (3)$$

where K_1, K_2, … K_a are the stepwise ligand protonation constants.

The merit of comparing pM values (pM = −log [M_f]) rather than stability constants of the metal complexes is that the pM values give repression to the influence of ligand basicity and metal chelate protonation. The calculation of [M_f] takes into consideration the protonation constants of the ligand and the stability constants of protonated metal complexes.[5] The larger the pM value, the higher the affinity of that ligand for the metal ion under the specified conditions. The relative order of the stability constants may change if a different set of conditions (concentration and pH) is used to calculate the pM values.

S3 Luminescence method for establishing solution hydration states. Luminescence lifetime data has been obtained for the Eu(III) complexes to determine the number of inner-sphere water molecules in the aqueous solution. The luminescence lifetime (τ) and the *q* value of Eu(III) complexes are shown in Table 2S. The luminescence lifetime (τ) has been determined in both H_2O and D_2O. The *q* value of Eu(III) complexes was calculated by the following equations (1S) and (2S)[6, 7]

$$q = 1.05[\tau_{H_2O}^{-1} - \tau_{D_2O}^{-1}] \qquad (1S)$$

$$q = 1.2[(\tau_{H_2O}^{-1} - \tau_{D_2O}^{-1}) - 0.25] \qquad (2S)$$

where *q* is the number of water molecules bound to metal ions, τ_{H_2O} is the luminescence half-life in H_2O solution and τ_{D_2O} is the luminescence half-life in D_2O solution.

S4 Variable-Temperature ^{17}O NMR Measurements. For the ^{17}O NMR measurements, the inversion recovery method was applied to measure longitudinal relaxation rates, $1/T_1$, and the Carr-Purcell-Meiboom-Gill spin-echo technique was used to obtain transverse relaxation rates, $1/T_2$. In order to eliminate magnetic susceptibility corrections to chemical shift, the solution was introduced into spherical glass containers fitting into ordinary 10-mm NMR tubes. From the measured ^{17}O NMR relaxation rates and angular frequencies of the Gd(III) containing solutions, $1/T_1$, $1/T_2$, and ω, and of the acidified water reference, $1/T_{1A}$, $1/T_{2A}$, and ω_A, one can calculate the reduced relaxation rates and chemical shift, $1/T_{1r}$, $1/T_{2r}$, and $\Delta\omega_r$:

$$\frac{1}{T_{1r}} = \frac{1}{P_m}\left[\frac{1}{T_1} - \frac{1}{T_{1A}}\right] = \frac{1}{T_{1m} + \tau_m} + \frac{1}{T_{1os}} \tag{3S}$$

$$\frac{1}{T_{2r}} = \frac{1}{P_m}\left[\frac{1}{T_2} - \frac{1}{T_{2A}}\right] = \frac{1}{\tau_m}\frac{T_{2m}^{-2} + \tau_m^{-1}T_{2m}^{-1} + \Delta\omega_m^2}{\left(\tau_m^{-1} + T_{2m}^{-1}\right)^2 + \Delta\omega_m^2} + \frac{1}{T_{2os}} \tag{4S}$$

$$\Delta\omega_r = \frac{1}{P_m}(\omega - \omega_A) = \frac{\Delta\omega_m}{\left(1 + \tau_m T_{2m}^{-1}\right)^2 + \tau_m^2\Delta\omega_m^2} + \Delta\omega_{os} \tag{5S}$$

P_m is the mole fraction of bound water.

$1/T_{2m}$ is the relaxation rates in the bound water.

$\Delta\omega_m$ is the chemical shift difference between bound water and bulk water.

$$\Delta\omega_m = \frac{g_L\mu_B S(S+1)B}{3k_B T}\frac{A}{\hbar} \tag{6S}$$

where g_L is the isotropic Landé g factor (g_L = 2.0 for Gd(III))

S is the electron spin (S = 7/2 for Gd(III))

$A/\hbar$ is the hyperfine or scalar coupling constant

B is the magnetic field

$$\frac{1}{T_{2m}} \cong \frac{1}{T_{2sc}} = \frac{S(S+1)}{3}\left(\frac{A}{\hbar}\right)^2\left[\tau_{1S} + \frac{\tau_{2S}}{1 + \omega_S^2\tau_{2S}^2}\right] \tag{7S}$$

where $1/\tau_{is} = 1/\tau_M + 1/T_{ie}$

$\Delta H^{\neq}$ and $\Delta S^{\neq}$ are the enthalpy and entropy of activation for the exchange process :

$$\frac{1}{\tau_m} = k_{ex} = \frac{k_B T}{h}\exp\left\{\frac{\Delta S^*}{R} - \frac{\Delta H^*}{RT}\right\} \tag{8S}$$

The ^{17}O longitudinal relaxation rates in Gd(III) solutions are dominated by the dipole-dipole and quadrupolar mechanisms, and are given by below :

$$\frac{1}{T_{1m}} = \left[\frac{1}{15}\left(\frac{\mu_0}{4\pi}\right)^2 \frac{\hbar^2\gamma_I^2\gamma_S^2}{r_{GdO}^6} S(S+1)\right]\left[6\pi_{d1} + 14\frac{\tau_{d2}}{1+\omega_S^2\tau_{d2}}\right] + \frac{3\pi^2}{10}\frac{2I+3}{I^2(2I-1)}\chi^2\left(1+\frac{\eta^2}{3}\right)\tau_R \qquad (9S)$$

where γ_I is the nuclear gyromagnetic ratio ($\gamma_I = -3.626\times10^7$ rad s^{-1} T^{-1} for ^{17}O), γ_{GdO} is the mean Gd(III)–O distance, I is the nuclear spin ($I = 5/2$ for ^{17}O), χ is the quadrupolar coupling constant, η an asymmetry parameter, and $\tau_{di} = \tau_M^{-1} + T_{ie}^{-1} + \tau_R^{-1}$. Using the quadrupolar coupling constant for acidified water, $\chi(1 + \eta^{2/3})^{1/2} = 7.58$ MHz, and estimating $r = 2.5$ Å is based on $[Gd(DTPA)]^{2-}$ crystal structure.[8, 9]

$$\tau_R = \tau_R^{298}\exp\left[\frac{E_R}{R}\left(\frac{1}{T} - \frac{1}{298.15}\right)\right] \qquad (10S)$$

E_R : activation energy

The outer-sphere contribution to $\Delta\omega_r$ has a similar temperature dependence to $\Delta\omega_m$ and is given by below, where C_{os} is an empirical constant.

$\Delta\omega_{os} = C_{os}\Delta\omega_m$ (11S)

S5 Proton relaxation enhancement (PRE) method. The characterization of the binding parameters consists in the determination of the enhancement factor ε^*, which is related to the measured R_{1obs}, according to the following relationship:

$$\varepsilon^* = \frac{R^*_{1obs} - R^*_{1d}}{R_{1obs} - R_{1d}} \qquad (12S)$$

The asterisk in equation (12S) indicated the presence in solution of the added macromolecule. The determination of the binding parameters K_A and n for the equilibrium:

$$\mathrm{GdL} + \mathrm{HSA} \underset{}{\overset{K_A}{\rightleftharpoons}} \mathrm{GdL{-}HSA}$$

$$K_A = \frac{[GdL - HSA]}{[GdL]_F [nHSA]_F} = \frac{[GdL \bullet HSA]}{([GdL]_T - [GdL - HSA])([nHSA]_T - [GdL - HSA])} \qquad (13S)$$

$$\varepsilon^* = \frac{[GdL - HSA]}{[GdL]_T} b + \frac{[GdL]_T - [GdL - HSA]}{[GdL]_T} \qquad (14S)$$

where [nHSA] represents the sites concentration, while the T and F subscripts refer to "total" and "free" species, respectively. By combining equations 13S and 14S to obtain equation 15S, which allows the non-linear fitting of the experimental data:

$$\varepsilon^* = (b-1)\frac{(K_A[GdL]_T + K_A[nHSA]_T + 1) - \sqrt{(K_A[GdL]_T + K_A[nHSA]_T + 1)^2 - 4K_A^2[nHSA][GdL]_T}}{2K_A[GdL]_T} + 1$$

(15S)

The former reports the change of ε^* as the $[\mathrm{HSA}]_T$ / $[\mathrm{GdL}]_T$ ratio increases, keeping $[\mathrm{GdL}]_T$ constant. The fitting of these experimental data allows the evaluation of b and of the product $K_A \times n$. In the M titration, in contrast, the ε^* values are measured in solutions containing a fixed HSA concentration and variable concentration of Gd(III) complexes. The data from this titration are often more conveniently analysed in the form of a Scatchard plot according to equation (16S)

$$r/[\mathrm{GdL}]_F = nK_A - rK_A \qquad (16S)$$

where r represents the molar binding ratio, *i.e.* [GdL-HSA]/$[\mathrm{HSA}]_T$. This ratio can be calculated when b is obtained from the E titration. In the case of a single class of binding sites, a plot of $r/[\mathrm{GdL}]_F$ versus r gives a straight line whose x–axis intercept is equal to n, while the slope corresponds to K_A.

References

1. C. F. G. C. Geraldes, A. M. Urbano, M. C. Alpoim, A. D. Sherry, K. T. Kuan, R. Rajagopalan, F. Maton and R. N. Muller, *Magn. Reson. Imaging*, 1995, **13**, 401-420.
2. J. L. Sudmeier and C. N. Reilley, *Anal. Chem.*, 1964, **36**, 1698-1706.
3. Y. M. Wang, C. H. Lee, G. C. Liu and R. S. Sheu, *J. Chem. Soc., Dalton Trans.*, 1998, **24**, 4113-4118.
4. W. P. Cacheris, S. C. Quay and S. M. Rocklage, *Magn. Reson. Imaging*, 1990, **8**, 467-481.
5. W. R. Harris, K. N. Raymond and F. L. Weitl, *J. Am. Chem. Soc.*, 1981, **103**, 2667-2675.
6. W. D. Horrocks, Jr. and D. R. Sudnick, *J. Am. Chem. Soc.*, 1979, **101**, 334-340.
7. A. Beeby, I. M. Clarkson, R. S. Dickins, S. Faulkner, D. Parker, L. Royle, A. S. D. Sousa, J. A. G. Williams and M. Woods, *J. Chem. Soc., Perkin Trans. 2*, 1999, 493-504.
8. M. R. Spirlet, J. Rebizant, J. F. Desreux and M. F. Loncin, *Inorg. Chem.*, 1984, **23**, 359-363.
9. J. J. Stezowski and J. L. Hoard, *Isr. J. Chem.*, 1984, **24**, 323-334.